J|A|C|S
ARTICLES
Published on Web 08/14/2002

Inter- and Intramolecular Spin Transfer in Molecular Magnetic Materials. Solid-State NMR Spectroscopy of Paramagnetic Metallocenium Ions

Henrike Heise,[1a] Frank H. Köhler,* Martin Herker,[1b] and Wolfgang Hiller[1b]

Contribution from the Anorganisch-chemisches Institut, Technische Universität München, D-85747 Garching, Germany

Received January 7, 2002. Revised Manuscript Received May 30, 2002

Abstract: To shed light on the interaction in molecule-based magnetic materials, the decamethylmetallocenium hexafluorophosphates, $[(C_5Me_5)_2M]^+$ $[PF_6]^-$ with M = Cr, Mn, Fe, Co, and Ni, as well as the tetracyanoethenides, $[(C_5Me_5)_2M]^+$ $[TCNE]^-$ with M = Cr, Mn, Fe, and Co, have been investigated in the solid state by using ^1H, ^{13}C, ^{19}F, and ^{31}P NMR spectroscopy under magic angle spinning (MAS). The isotropic ^{13}C and ^1H NMR signals cover ranges of about 1300 and 500 ppm, respectively. From the shift anisotropies of the ring carbon signal of the $[(C_5Me_5)_2M]^+$ cations, the total unpaired electron spin density in the ligand π orbitals has been calculated; it amounts up to 36% (M = Ni) and is negative for M = Cr, Mn, and Fe. The radical anion of $[(C_5Me_5)_2M]^+$ $[TCNE]^-$ shifts the ^{13}C NMR signals of all $[(C_5Me_5)_2M]^+$ cations to high frequency, which establishes transfer of positive spin density from the anions to the cations. The ^{19}F and ^{31}P NMR signals of the paramagnetic salts $[(C_5Me_5)_2M]^+$ $[PF_6]^-$ are shifted up to 13.5 ppm relative to diamagnetic $[(C_5Me_5)_2Co]^+$ $[PF_6]^-$. The signs of these shifts are the same as those of the π spin density in $[(C_5Me_5)_2M]^+$. After consideration of interionic ligand- and metal-centered dipolar shifts, this establishes cation−anion spin delocalization. The mixed crystals $[(C_5Me_5)_2M_xCo_{1-x}]^+$ $[PF_6]^-$ have been prepared for M = Cr and Ni. They are isostructural with $[(C_5Me_5)_2Co]^+$ $[PF_6]^-$ whose single-crystal structure has been determined by X-ray diffraction. The ^{13}C, ^{19}F, and ^{31}P MAS NMR spectra of the mixed crystals show that the respective two closest paramagnetic ions in the lattice delocalize spin density to $[(C_5Me_5)_2Co]^+$, $[(C_5Me_5)_2Ni]^+$, and $[PF_6]^-$. In $[(C_5Me_5)_2M]^+$, about 10^{-4} au per carbon atom are transferred.

Introduction

In many magnetic materials that are derived from neutral molecules or from ions, the interaction *between* discrete paramagnetic species plays an important role for the bulk magnetic properties. Prominent examples of neutral molecules are organic radicals, which in the solid state and at low temperature experience spontaneous magnetization.[2] The magnetic interaction between two adjacent radicals is particularly simple if it is reduced to the interaction between two unpaired electron spins. When two independent spins (each localized in an orbital) are brought in close proximity, they line up antiparallel to yield a spin singlet. If the interaction (through orbital overlap) is weak, it is known as antiferromagnetic interaction; if it is strong, we have a bond like that of the H_2 molecule. By analogy to the bonding model of H_2, magnetic interaction is hence described by a spin exchange model, the McConnell-I mechanism.[3]

This model does not only explain intermolecular antiferromagnetic but also ferromagnetic interactions, when delocalization of unpaired electron spin density from the spin center to the periphery of the engaged species is taken into account. The two scenarios are illustrated in Figure 1: (i) If in molecule **A** (Figure 1a), the spin occupies a molecular orbital (MO) that extends to site **A′**, positive spin density is delocalized directly to site **A′**. Positive spin density means that the associated magnetic moment is parallel to the net spin moment of the molecule (arrows pointing up). When two molecules **A** are arranged as in Figure 1b and when they approach so that sites **A′** interact, the spin exchange model would lead to antiferromagnetic coupling (assuming a negative coupling constant[3]). (ii) If in molecule **B** (Figure 1c), direct delocalization to site **B′** is negligible, spin polarization may dominate. In this case, the unpaired electron of **B** polarizes a bonding electron pair that connects **B** and **B′**. The net effect is an increase of positive spin density at **B** and negative spin density (arrow pointing

* Address correspondence to this author. E-mail: F.H.Koehler@lrz.tu-muenchen.de.

(1) (a) New address: Max-Planck-Institute for Biophysical Chemistry, Am Fassberg M, D-37077 Göttingen, Germany. (b) Single-crystal structure analysis.

(2) (a) *Magnetic Properties of Organic Materials*; Lahti, P. M., Ed.; Marcel Dekker: New York, 1999. (b) *Molecular Magnetism*; Itoh, K., Kinoshita, M., Eds.; Kodasha: Tokyo and Gordon and Breach Science Publishers: Australia, 2000. (c) *Magnetism: Molecules to Materials, Models and Experiments*; Miller, J. S., Drillon, M., Eds.; Wiley-VCH: Weinheim, Germany, 2001. (d) Veciana, J.; Iwamura, H. *MRS Bull.* **2000**, *25*, 41−45. (e) Nakatsuji, S.; Anzei, H. *J. Mater. Chem.* **1997**, *7*, 2161−2174. (f) Kinoshita, M. In *Handbook of Organic Conductive Molecules and Polymers*; Nalva, H. S., Ed.; Wiley: Chichester, U.K., 1997; Vol. 1, pp 781−800. (g) *From Molecular Assemblies to the Devices*; Coronado, E., Delhaès, P., Gatteschi, D., Eds.; Kluver: Dodrecht, The Netherlands, 1996. (h) Neshide, H. *Adv. Mater.* **1995**, *7*, 937−941. (i) Rajca, A. *Chem. Rev.* **1994**, *94*, 871−893.

(3) (a) McConnell, H. M. *J. Chem. Phys.* **1963**, *39*, 1910. (b) Novoa, J. J.; Deumal, M. *Struct. Bonding (Berlin)* **2001**, *100*, 33.

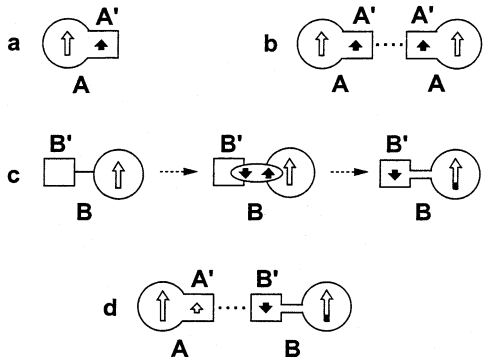

Figure 1. The McConnell-I mechanism of spin alignment. (a) Delocalization of positive spin to the peripheral site **A′** of molecule **A**. (b) Decrease of the distance between the sites **A′** leads to antiferromagnetic interaction. (c) Induction of negative spin to the peripheral site **B′** of molecule **B**. (d) Intermolecular ferromagnetic interaction between two molecules **A** and **B**, after decreasing the distance between sites **A′** and **B′**.

down) at site **B′**. As shown in Figure 1d, molecule **B** may be combined with molecule **A** in such a way that positive spin at site **A′** interacts with negative spin density at site **B′**. Then the spin exchange model would lead to ferromagnetic coupling. In a more detailed treatment, additional contributions to the interaction must be considered.[3b]

With these two scenarios in mind, the first question is the following: How can sites with negative spin density be determined in discrete molecules? The perhaps best-studied radicals in terms of spin density distribution are nitronylnitroxides,[4] and the most suitable methods are EPR and NMR spectroscopies as well as polarized neutron diffraction. The strengths and weaknesses of these methods have been discussed.[4b,c] The often small spin densities at the periphery of radicals, which are still relevant for the McConnell-I mechanism, cannot be resolved by polarized neutron diffraction. As for EPR spectroscopy, spin distributions of radicals in the pseudo-gas phase can be determined,[4c] but usually electron relaxation does not allow studying pure radicals in the magnetically interesting state, that is, the solid state. This problem can be overcome by solid-state NMR spectroscopy, which has afforded precise spin maps of, for example, nitronylnitroxides including the spin signs.[4b] From the signs, *intra*molecular spin delocalization can be analyzed.

A second question that comes to mind when considering the McConnell-I mechanism is the following: What are the *inter*molecular effects between pairs of molecules such as **A····A** and **A····B** in Figures 1b and 1d? Is the spin density of a given radical changed by adjacent radicals? The above-mentioned nitronylnitroxides are not well suited for answering these questions, because referencing the data of interacting radicals to those of isolated radicals fails; the latter do not yield NMR signals owing to slow electron relaxation.

Better candidates for the study of intermolecular interactions are the paramagnetic decamethylmetallocenium salts $[(C_5Me_5)_2M]^+ X^-$. These compounds were expected to yield solid-state NMR spectra as do neutral metallocenes.[5] We reasoned that with this method intermolecular changes of the spin

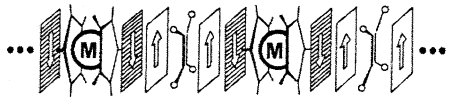

Figure 2. Model of a $[(C_5Me_5)_2M]^+$ $[TCNE]^-$ stack showing two formula units. The rectangular planes represent the π clouds at TCNE (nonshaded) and at the periphery of the metallocenium ions (shaded); the arrows reflect the sign of the electron spin density. Open circles are CN groups.

distribution might be visible because the paramagnetic sandwich ion $[(C_5Me_5)_2M]^+$ would be less influenced by its surrounding when the counterion X^- is PF_6^- [6] rather than tetracyanoethenide, $[TCNE]^-$, or a similar planar radical anion. The solid-state structure of $[(C_5Me_5)_2M]^+$ $[TCNE]^-$ [7] consists of stacks made up from alternating anions and cations as visualized in Figure 2. The structural model emphasizes the fact that spin-containing areas of neighboring species lie on top of one another, thereby realizing a scenario, which is required by the McConnell-I mechanism to generate ferromagnetic interaction. This follows from the comparison of Figures 1 and 2. Site **A′** in Figure 1d corresponds to the π system of $[TCNE]^-$ or the nonshaded planes in Figure 2, while site **B′** corresponds to the π systems of the metallocene ligands or the shaded planes in Figure 2. It will be discussed below that the spin density at $[(C_5Me_5)_2M]^+$ can also be inverted.

Compounds of the type $[(C_5Me_5)_2M]^+$ $[TCNE]^-$ have inspired many research groups because they do not only experience ferromagnetic interaction but also spontaneous magnetization at low temperature.[8] While this has been one of the triggers of the ongoing quest for molecular magnetic materials,[9] the interaction mechanism has been under debate for quite some time.[10] Besides the McConnell-I mechanism already mentioned and worked out in detail for the metallocenium ions by Kollmar and Kahn,[10c,d,g] there is also the McConnell-II mechanism[10a] discussed by Miller and Epstein[10b] and adequately implemented by Tchougreeff.[10e,f] The latter mechanism implies the back charge transfer from $[(C_5Me_5)_2M]^+$ $[TCNE]^-$ to an excited high-spin state which is admixed to the ground state. Strong evidence for the McConnell-I mechanism came from NMR experiments, which in the case of metallocenium cations were limited to solutions.[11] From the sign of the paramagnetically induced signal shifts, it was concluded that the spin density on the cyclopen-

(4) (a) Schweizer, J.; Ressouche, E. in ref 2c, pp 324−355. (b) Heise, H.; Köhler, F. H.; Mota, F.; Novoa, J. J.; Veciana, J. *J. Am. Chem. Soc.* **1999**, *121*, 9659−9667. (c) Cirujeda, J.; Vidal-Gancedo, J.; Jürgens, O.; Mota, F.; Novoa, J. J.; Rovira, C.; Veciana, J. *J. Am. Chem. Soc.* **2000**, *122*, 11393−11405.

(5) (a) Blümel, J.; Herker, M.; Hiller, W.; Köhler, F. H. *Organometallics* **1996**, *15*, 3474−3476. (b) Köhler, F. H.; Xie, X. *Magn. Reson. Chem.* **1997**, *35*, 487−492. (c) Heise, H.; Köhler, F. H.; Xie, X. *J. Magn. Reson.* **2001**, *150*, 198−206.

(6) Robbins, J. L.; Edelstein, N.; Spencer, B.; Smart, J. C. *J. Am. Chem. Soc.* **1982**, *104*, 1882−1893.

(7) Miller, J. S.; Calabrese, J. C.; Rommelmann, H.; Chittipeddi, S. R.; Zhang, J. H.; Reiff, W. M.; Epstein, A. J. *J. Am. Chem. Soc.* **1987**, *109*, 769−781.

(8) (a) Miller, J. S.; Calabrese, J. C.; Epstein, A. J.; Biegelow, R. W.; Zang, J. H.; Reiff, W. M. *J. Chem. Soc., Chem. Commun.* **1986**, 1026−1028 (b) Miller, J. S.; Epstein, A. J. *J. Am. Chem. Soc.* **1987**, *109*, 3850−3855. (c) Miller, J. S.; Epstein, A. J.; Reiff, W. M. *Chem. Rev.* **1988**, *88*, 201−220.

(9) Recent review: (a) Miller, J. S. *Inorg. Chem.* **2000**, *39*, 4392−4408. Recent relevant metallocenium compounds: (b) Da Gama, V.; Belo, D.; Rabaca, S.; Santos, I. C.; Alves, H.; Waerenborgh, J. C.; Duarte, M. T.; Henriques, R. T. *Eur. J. Inorg. Chem.* **2000**, 2101−2110. (c) Kaul, B. B.; Sommer, R. D.; Noll, B. C.; Yee, G. T. *Inorg. Chem.* **2000**, *39*, 865−868. (d) Yee, G. T.; Whitton M. J.; Sommer, R. D.; Frommen, C. M.; Reiff, W. M. *Inorg. Chem.* **2000**, *39*, 1874−1877.

(10) (a) McConnel, H. M. *Proc. R. A. Welch Found. Chem. Res.* **1967**, *11*, 144. (b) Miller, J. S.; Epstein, A. J. *J. Am. Chem. Soc.* **1987**, *109*, 3850−3855. (c) Kollmar, C.; Couty, M.; Kahn, O. *J. Am. Chem. Soc.* **1991**, *113*, 7994−8005 (d) Kollmar, C.; Kahn, O. *J. Chem. Phys.* **1992**, *96*, 2988−2997. (e) Tchougreeff, A. L. *J. Chem. Phys.* **1992**, *96*, 6026−6032. (f) Tchougreeff, A. L.; Misurkin, I. A. *Phys. Rev. B: Condens. Matter* **1992**, *46*, 5357−5365. (g) Kollmar, C.; Kahn, O. *J. Chem. Phys.* **1993**, *98*, 453−472.

(11) (a) Blümel, J.; Hebendanz, N.; Hudeczek, P.; Köhler, F. H.; Strauss, W. *J. Am. Chem. Soc.* **1992**, *114*, 4223−4230. (b) Gattinger, I.; Herker, M. A.; Hiller, W.; Köhler, F. H. *Inorg. Chem.* **1999**, *38*, 2359−2368.

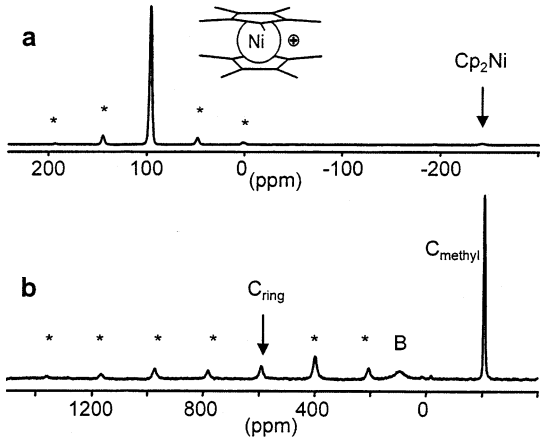

Figure 3. ^{1}H (a) and ^{13}C (b) MAS NMR spectra of $[(C_5Me_5)_2Ni]^+$ $[PF_6]^-$ (temperature: 310.5 K, spinning rate: 14.5 kHz). Spinning sidebands are marked by asterisks, B is the background signal of the probehead. The proton NMR signal of the internal temperature standard Cp_2Ni is marked by an arrow.

tadienyl ligands is negative when the metal is Cr, Mn, and Fe, while it is positive for Ni. This corresponds to what has been claimed[10c,d,g] for ferro- and antiferromagnetic interaction, respectively, between $[(C_5Me_5)_2M]^+$ and $[TCNE]^-$. The NMR analysis may suffer from errors because of dipolar signal shifts discussed in more detail below. These errors were avoided by introducing ethyl[11a] and bicyclic[11b] spectator substituents in the metallocenium cations. A drawback was that the compounds were slightly different from those showing spontaneous magnetization and that the spin density was not analyzed quantitatively.

For decamethylferrocenium ion, the McConnell-I mechanism has been confirmed very recently by Schweizer et al. who used polarized neutron diffraction.[12] They were able to directly observe negative spin density on the ring carbon atoms of both ligands of the cation $[(C_5Me_5)_2Fe]^+$, which corresponded to 5% of an unpaired electron.[12a] A calculation that allowed interaction with positive spin density at the central carbon atoms of $[TCNE]^-$ (33% of an unpaired electron[12b]) gave an interaction constant, which was ferromagnetic albeit somewhat smaller than found experimentally.

In the present study, we demonstrate that the *intra*molecular spin transfer to the ligands of metallocenium ions can be determined quantitatively (and independently from the isotropic shift procedure[11]) with the help of solid-state NMR spectroscopy. This is accompanied by switching from magnetically isolated species studied previously to molecular solids that are more appropriate from the materials' point of view. In particular, it will be shown that even *inter*molecular effects on the spin distribution can be studied quite generally by observing nuclei ^{1}H, ^{13}C, ^{19}F, and ^{31}P in the decamethylmetallocenium salts $[(C_5Me_5)_2M]^+$ $[TCNE]^-$ and $[(C_5Me_5)_2M]^+$ $[PF_6]^-$.

Results

^{1}H and ^{13}C MAS NMR Spectra. Figure 3 shows the ^{1}H (a) and ^{13}C (b) MAS NMR spectra of solid $[(C_5Me_5)_2Ni]^+$ $[PF_6]^-$ ($S = 1/2$). The proton NMR spectrum exhibits a single signal

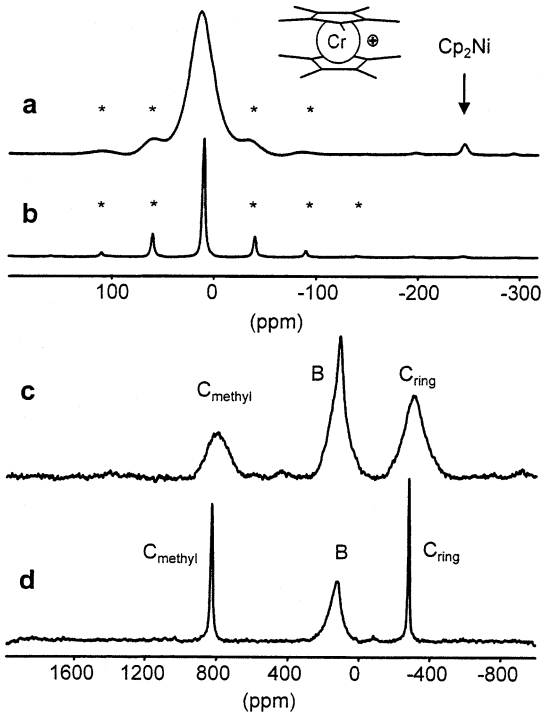

Figure 4. ^{1}H (a and b) and ^{13}C (c and d) MAS NMR spectra of $[(C_5Me_5)_2Cr]^+$ $[PF_6]^-$ (a and c) and of $[(C_5Me_5)_2Cr]^+$ $[TCNE]^-$ (b and d) (temperatures: 308 K (a and c) and 309 K (b and d), spinning rates: 14.5 kHz (a and c) and 15 kHz (b and d)). Spinning sidebands are marked by asterisks, B is the background signal of the probehead. The proton NMR signal of the internal temperature standard Cp_2Ni is marked by an arrow.

with a large positive shift of 95.9 ppm at 310 K. The half-width of the signal, $\Delta\nu_{1/2}$, is 850 Hz, and the spinning sidebands cover a range of about 200 ppm. The ^{13}C MAS NMR spectrum has two signals at 590 ppm ($\Delta\nu_{1/2} = 840$ Hz) and at -208 ppm ($\Delta\nu_{1/2} = 380$ Hz). While the ^{13}C NMR signal at low frequency is not accompanied by spinning sidebands at the spinning speed of 14.5 kHz, the high-frequency signal exhibits a large spinning sideband manifold covering a range of about 1500 ppm. The intensities of the spinning sidebands reflect an anisotropic powder pattern characteristic for an axially symmetric shift tensor[13] with the isotropic line at the center of mass of the anisotropic signal. The signal assignment is based on the spin delocalization mechanism and the spinning sideband patterns. This will be outlined in the Discussion; it applies for all other spectra. Temperature-dependent ^{13}C MAS NMR spectra showed that from ambient temperature up to about 100 °C the signal shifts follow the Curie law (Figure SI1, Supporting Information)

The ^{1}H and ^{13}C MAS NMR spectra of solid $[(C_5Me_5)_2Cr]^+$ $[PF_6]^-$ ($S = 3/2$) (Figure 4a and 4c) featured signals, which were much broader than those of the nickel analogue. When the counterion $[PF_6]^-$ was replaced by $[TCNE]^-$ ($S = 1/2$) (Figure 4b and 4d), the proton signal shifted from 13.6 to 10.0 ppm, the ring carbon signal from -309 to -289 ppm, and the methyl carbon signal from 800 to 824 ppm. In addition, a striking signal narrowing by factors of 4, 11, and 17, respectively, was observed. As will be outlined later, the mechanism of the spin delocalization changes on going from the nickel to the chromium derivative (and likewise to the manganese and iron derivative, see below). Therefore, the shift signs of the carbon signals of $[(C_5Me_5)_2Cr]^+$ are opposite to those of $[(C_5$-

(12) (a) Schweizer, J.; Bencini, A.; Carbonera, C.; Epstein, A. J.; Golhen, S.; Lelièvre-Berna, E.; Miller, J. S.; Ouahab, L.; Pontillon, Y.; Ressouche, E.; Zheludev, A. *Polyhedron* **2001**, 1771−1778. (b) Zheludev, A.; Grand, A.; Ressouche, E.; Schweizer, J.; Morin, B. G.; Epstein, A. J.; Dixon, D. A.; Miller, J. S. *J. Am. Chem. Soc.* **1994**, *116*, 7243−7249.

(13) Herzfeld, J.; Berger, A. E. *J. Chem. Phys.* **1980**, *73*, 6021−6030.

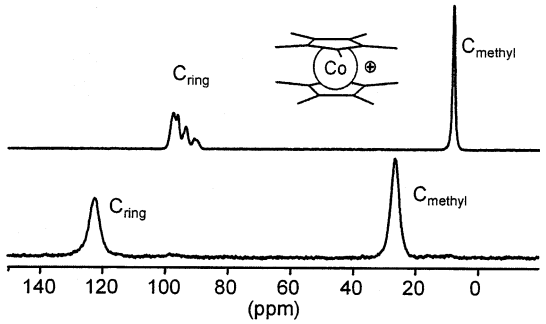

Figure 5. ^{13}C CP MAS NMR spectra of $[(C_5Me_5)_2Co]^+$ $[PF_6]^-$ (a) and $[(C_5Me_5)_2Co]^+$ $[TCNE]^-$ (b).

$Me_5)_2Ni]^+$, and no sideband patterns are visible in traces c and d of Figure 4.

The $[(C_5Me_5)_2Mn]^+$ ($S = 1$) and $[(C_5Me_5)_2Fe]^+$ ($S = 1/2$) cations as $[PF_6]^-$ and $[TCNE]^-$ salts, respectively, gave similar spectra (Figures SI2, SI3, SI4, and SI5, Supporting Information). Thus, at spinning speeds higher than 13 kHz, spinning sidebands were only observed in the ^{1}H MAS NMR spectra, and substitution of $[PF_6]^-$ for $[TCNE]^-$ led to changes of the signal shifts and half-widths, although the signal narrowing was less pronounced than for the chromium derivative. The compound $[(C_5Me_5)_2Mn]^+$ $[TCNE]^-$ is thermolabile[14] while it is more stable when the counterion is $[PF_6]^-$.[6] This was confirmed by the ^{13}C MAS NMR spectra, which showed signals of decomposition products for the $[TCNE]^-$ but not for the $[PF_6]^-$ salt.

When the cation of $[(C_5Me_5)_2M]^+$ $[X]^-$ was diamagnetic, the replacement of $[X]^- = [PF_6]^-$ by the radical anion $[TCNE]^-$ also entailed changes of the solid-state NMR signal shifts. This is illustrated by the ^{13}C MAS NMR spectra of $[(C_5Me_5)_2Co]^+$ salts in Figure 5. The methyl and ring carbon signals of the $[PF_6]^-$ salt appear at 8.1 and 95.3 ppm, respectively, the latter signal featuring second-order dipolar coupling to the quadrupolar nucleus ^{59}Co.[15] In the $[TCNE]^-$ salt at 298 K, these signals are shifted to high frequencies by 18.8 and 26.3 ppm, respectively. A variable-temperature MAS NMR study revealed that the shifts are inversely proportional to the absolute temperature as expected from the Curie law (Figure SI6, Supporting Information). This is a clear indication that these signal shifts are due to interactions with unpaired electrons (see Discussion).

^{31}P and ^{19}F MAS NMR Spectra. In Figure 6, the ^{31}P MAS NMR spectra of the decamethylmetallocenium compounds $[(C_5Me_5)_2M]^+$ $[PF_6]^-$ with M = Ni, Co, Fe, Mn, and Cr are displayed. For the diamagnetic salt $[(C_5Me_5)_2Co]^+$ $[PF_6]^-$ (Figure 6b), the spectrum consists of a well-resolved septet at 144.1 ppm ($\Delta\nu_{1/2} = 150$ Hz) because of scalar coupling to six equivalent ^{19}F atoms with the coupling constant $J(^{31}P, ^{19}F) = 720 \pm 10$ Hz, which is in accord with literature data.[16] In the ^{31}P NMR spectrum of $[(C_5Me_5)_2Ni]^+$ $[PF_6]^-$ (Figure 6a), the septet structure of the signal is maintained, the half-width of the signal has increased to 450 Hz, and there is a signal shift of 11 ppm to high frequency with respect to the diamagnetic signal of the cobaltocenium salt. When the metal M in $[(C_5Me_5)_2M]^+$ $[PF_6]^-$ is Fe, Mn, and Cr, the ^{31}P MAS NMR spectra in Figure

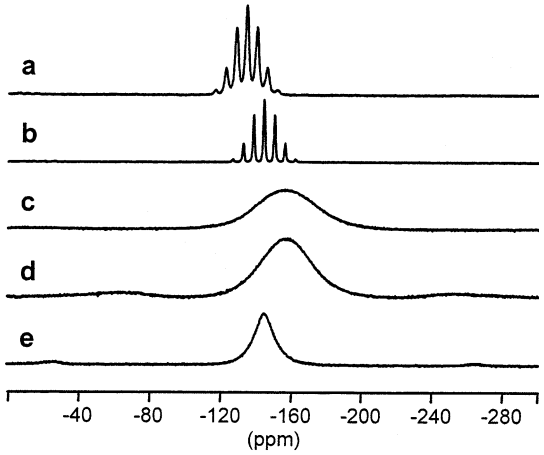

Figure 6. ^{31}P MAS NMR spectra of $[(C_5Me_5)_2M]^+$ $[PF_6]^-$ with M = Ni (a), Co (b), Fe (c), Mn (d), Cr (e) (temperatures: 307−315 K, spinning rate: 14.5 kHz).

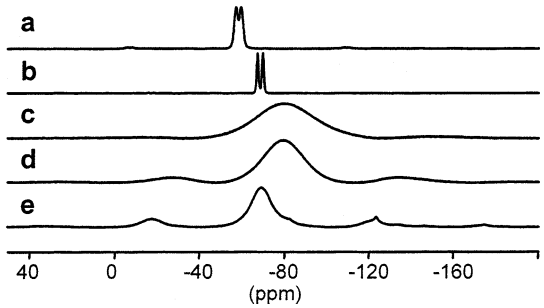

Figure 7. ^{19}F MAS NMR spectra of $[(C_5Me_5)_2M]^+$ $[PF_6]^-$ with M = Ni (a), Co (b), Fe (c), Mn (d), Cr (e) (temperatures: 307−315 K, spinning rate: 14.5 kHz).

6c, 6d, and 6e, respectively, show broad isotropic signals ($\Delta\nu_{1/2} = 4.8$, 4.1, and 1.7 kHz, respectively) without multiplet structure. These signals are shifted to low frequency relative to $[(C_5Me_5)_2Co]^+$ $[PF_6]^-$.

The ^{19}F MAS NMR spectra of all $[(C_5Me_5)_2M]^+$ $[PF_6]^-$ salts (Figure 7) exhibit a single isotropic signal. In $[(C_5Me_5)_2Ni]^+$ $[PF_6]^-$ and $[(C_5Me_5)_2Co]^+$ $[PF_6]^-$ (Figure 7a and 7b, respectively), it is split into a doublet, thus confirming the ^{31}P, ^{19}F coupling. When going from the diamagnetic cobalt to the paramagnetic nickel compound, the signal half-width roughly doubles, while the signals of $[(C_5Me_5)_2Fe]^+$ $[PF_6]^-$, $[(C_5Me_5)_2Mn]^+$ $[PF_6]^-$, and $[(C_5Me_5)_2Cr]^+$ $[PF_6]^-$ are too broad to observe the coupling (Figure 7c and 7d, respectively). A high-frequency shift of 10.7 ppm was found for the ^{19}F NMR signal of $[(C_5Me_5)_2Ni]^+$ $[PF_6]^-$ relative to $[(C_5Me_5)_2Co]^+$ $[PF_6]^-$, whereas the signals of $[(C_5Me_5)_2Fe]^+$ $[PF_6]^-$, $[(C_5Me_5)_2Mn]^+$ $[PF_6]^-$, and $[(C_5Me_5)_2Cr]^+$ $[PF_6]^-$ are shifted to low frequencies by amounts proportional to those of the corresponding ^{31}P NMR signals.

Mixed Crystals $[(C_5Me_5)_2M_xCo_{1-x}]^+$ $[PF_6]^-$ (M = Ni, Cr). To probe site-selective effects on the NMR spectra of solid paramagnetic metallocenium ions, $[(C_5Me_5)_2Ni]^+$ $[PF_6]^-$ and $[(C_5Me_5)_2Cr]^+$ $[PF_6]^-$ were cocrystallized with diamagnetic $[(C_5Me_5)_2Co]^+$ $[PF_6]^-$. The ratios were Ni/Co = 9/1 and 3/2 leading to $[(C_5Me_5)_2Ni_xCo_{1-x}]^+$ $[PF_6]^-$ ($x = 0.9$ and 0.6, respectively) as well as Cr/Co = 4/1 and 3/7 leading to $[(C_5Me_5)_2Cr_xCo_{1-x}]^+$ $[PF_6]^-$ ($x = 0.8$ and 0.3, respectively). Figure 8 demonstrates how the ^{13}C MAS NMR spectrum of $[(C_5Me_5)_2Co]^+$ $[PF_6]^-$ (Figure 8c) is affected by the presence of $[(C_5Me_5)_2Ni]^+$ $[PF_6]^-$

(14) Yee, G. T.; Manriquez, J. M.; Dixon, D. A.; McLean, R. S.; Groski, D. M.; Flippen, R. B.; Narayan, K. S.; Epstein, A. J.; Miller, J. S. *Adv. Mater.* **1991**, *3*, 309−311.
(15) Heise, H.; Köhler, F. H.; Brouwer, E.; Harris, R. K.; Steuernagel, S. *Magn. Reson. Chem.* **1999**, *37*, 573−578.
(16) (a) Latscha, H. P. *Z. Naturforsch., B* **1968**, *23*, 139−144. (b) Jander, J.; Börner, D.; Engelhardt, U. *Liebigs Ann. Chem.* **1969**, *726*, 19−24.

Table 1. ^{13}C, ^{19}F, and ^{31}P MAS NMR Signal Shifts and Intensities of the $[(C_5Me_5)_2Co]^+$ and $[PF_6]^-$ Ions in the Mixed Crystals $[(C_5Me_5)_2M_xCo_{1-x}]^+$ $[PF_6]^-$

paramagnetic center M	x	nucleus	signal shift[a], *exptl/theor intensity*[b]	$\Delta\delta_{av}$[d]
Ni	0.9	^{13}C	13.8, *0.81/0.81*; 7.0, *0.19/0.18*;[c], [c]*/0.01*	
		^{19}F	−58.0, *0.8/0.81*; −62.6, *0.2/0.18*;[c], [c]*/0.01*	
		^{31}P	−133.4, *0.8/0.81*; −139.2, *0.2/0.18*;[c], [c]*/0.01*	
	0.6	^{13}C	13.8, *0.32/0.36*; 6.9, *0.47/0.48*; 0.0, *0.21/0.16*	6.9
		^{19}F	−57.5, *0.3/0.36*; −62.6, *0.5/0.48*; −67.0, *0.2/0.16*	4.6
		^{31}P	−132.0, *0.4/0.36*; −137.9, *0.5/0.48*; −143.5, *0.1/0.16*	5.8
Cr	0.8	^{13}C	−8.2, *0.64/0.64*; −4.2, *0.27/0.32*; 0.0, *0.09/0.04*	
	0.3	^{13}C	−9.4, *0.10/0.09*; −5.1, *0.45/0.42*; −0.4, *0.45/0.49*	−4.4

[a] In ppm relative to pure $[(C_5Me_5)_2Co]^+$ $[PF_6]^-$. [b] Normalized values. [c] Not observed. [d] Change of the signal shift per paramagnetic neighboring cation, average of all measured shift differences of a given nucleus.

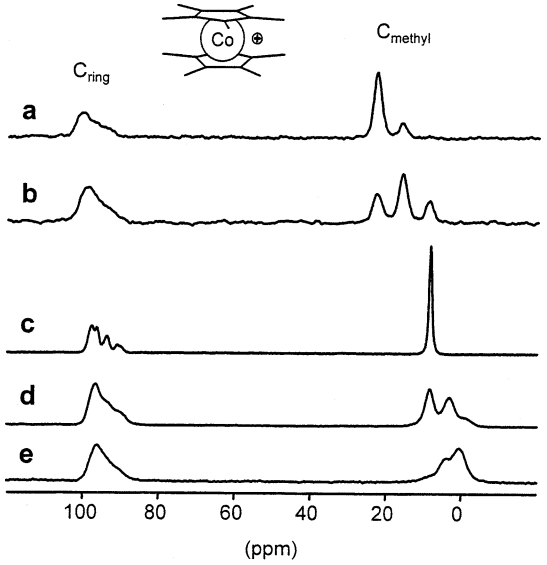

Figure 8. ^{13}C CP MAS NMR spectra of the $[(C_5Me_5)_2Co]^+$ cation in the mixed crystals. Traces a and b: $[(C_5Me_5)_2Ni_xCo_{1-x}]^+$ $[PF_6]^-$ with $x = 0.9$ (a) and 0.6 (b). Trace c: pure $[(C_5Me_5)_2Co]^+$ $[PF_6]^-$. Traces d and e: $[(C_5Me_5)_2Cr_xCo_{1-x}]^+$ $[PF_6]^-$ with $x = 0.3$ (d) and 0.8 (e).

(Figure 8a and 8b) and $[(C_5Me_5)_2Cr]^+$ $[PF_6]^-$ (Figure 8d and 8e). The signals of the methyl and ring carbon atoms are both broadened, but the most striking feature is the splitting of the methyl carbon signal. For instance, three signals at 22.5, 15.6, and 8.7 ppm with an intensity ratio of 0.32/0.47/0.21 were found when x was 0.6. Similar signal splittings were observed for other mixed crystals (Table 1). All patterns can be explained by assuming that the shift of the methyl signals is perturbed by two nearest-neighbor cations and that each paramagnetic neighbor leads to mean shifts of 6.9 ppm and −4.4 ppm for the salts containing $[(C_5Me_5)_2Ni]^+$ and $[(C_5Me_5)_2Cr]^+$, respectively. When $[(C_5Me_5)_2Ni]^+$ and $[(C_5Me_5)_2Cr]^+$ occupy random cation positions in the crystal lattice, the probability of finding two, one, and no paramagnetic neighbor next to $[(C_5Me_5)_2Co]^+$ corresponds to the binominal distribution, that is, to $x^2/2x(1-x)/(1-x)^2$, respectively. The theoretical signal intensities, which are also given in Table 1, are in good agreement with the experimental ones. As for the signal of the ring carbon atoms, the splitting pattern near 95 ppm (because of second-order dipolar coupling) is smeared out and prevents a reliable analysis of chemical shift changes.

The methyl carbon signal of $[(C_5Me_5)_2Ni]^+$ was narrow enough to observe a corresponding signal splitting for $[(C_5Me_5)_2Ni_xCo_{1-x}]^+$ $[PF_6]^-$ (Figure SI7). At 313 K, the signal shifts were −222, −214, and −207 ppm when x was 0.6, 0.9, and 1.0, respectively, which corresponds to an average shift of 7.5 ppm to high frequency per paramagnetic neighbor. Because of large signal widths, the expected splittings of other signals of the paramagnetic cations in the two mixed-crystal series could not be observed.

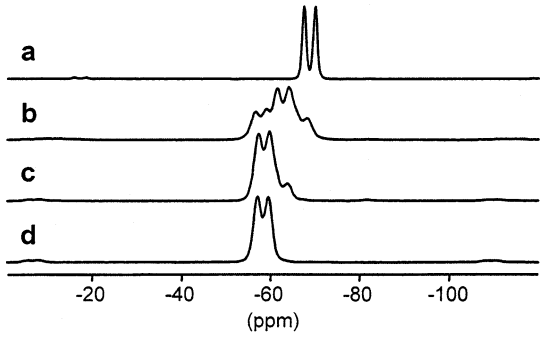

Figure 9. ^{19}F MAS NMR spectra of the mixed crystals $[(C_5Me_5)_2Ni_xCo_{1-x}]^+$ $[PF_6]^-$ with $x = 0.0$ (a), 0.6 (b), 0.9 (c), and 1.0 (d) (temperatures: 307−315 K, spinning rate: 14.5 kHz).

Corresponding signal splittings were observed in the ^{19}F and ^{31}P MAS NMR spectra of $[(C_5Me_5)_2Ni_xCo_{1-x}]^+$ $[PF_6]^-$ while in the chromium analogue the signal widths were too large (cf. Figures 6 and 7). In Figure 9, the ^{19}F MAS NMR spectra of the mixed crystals $[(C_5Me_5)_2Ni_xCo_{1-x}]^+$ $[PF_6]^-$ are compared to those of the pure $[(C_5Me_5)_2Co]^+$ and $[(C_5Me_5)_2Ni]^+$ salts. The doublet signal of $[(C_5Me_5)_2Co]^+$ $[PF_6]^-$ splits into a feature of three not completely resolved doublets that are equidistant in the error limits. Again, the intensity distribution agrees well with the binomial distribution (Table 1). The ^{31}P MAS NMR signal of $[(C_5Me_5)_2Ni_{0.6}Co_{0.4}]^+$ $[PF_6]^-$ (Figure SI8, Supporting Information) appears as a nine-line multiplet, which results from three overlapping heptets at −132.0, −137.9, and −143.5 ppm, respectively. Accidentally, at the magnetic field of 7.05 T, the signal shift differences of 5.9 ppm correspond to roughly half the ^{31}P, ^{19}F coupling constant. Analysis of the data for $x = 0.6$ and 0.9 confirms the ^{13}C and ^{19}F NMR results (Table 1).

The ^1H MAS NMR signal widths of $[(C_5Me_5)_2Ni_xCo_{1-x}]^+$ $[PF_6]^-$ prevented the resolution of the expected signal splitting (Figure SI9, Supporting Information). The effect of the paramagnetic next-neighbor cations was however obvious from the signal shifts. Thus, at 308 K the signal of $[(C_5Me_5)_2Co]^+$ moved from 2.1 to 1.3 ppm and 0.9 ppm when x was 0, 0.6, and 0.9, respectively. The signal shifts of $[(C_5Me_5)_2Ni]^+$ were 97.8 and 97.0 ppm for $x = 0.6$ and 0.9, respectively.

Crystal Structures. For the interpretation of intermolecular paramagnetic signal shifts, the arrangement of anions and cations in the crystal lattice and the interion distances were of interest. Therefore, $[(C_5Me_5)_2Co]^+$ $[PF_6]^-$ was investigated by single-

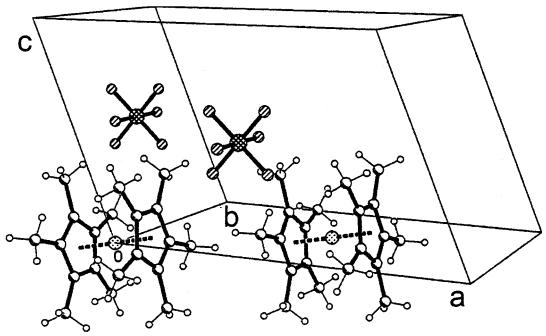

Figure 10. Crystallographic unit cell of $[(C_5Me_5)_2Co]^+$ $[PF_6]^-$ showing two selected ion pairs.

crystal X-ray analysis as a representative example of the decamethylmetallocenium hexafluorophosphates. The compound crystallizes in the monoclinic space group *C*2/*m* with two anions and cations per unit cell (Figure 10). The cell parameters at 199 K are $a = 14.05$ Å, $b = 8.90$ Å, $c = 9.12$ Å, and $\beta = 112.72$ Å. A comparison of the powder X-ray diffractograms of all compounds $[(C_5Me_5)_2M]^+$ $[PF_6]^-$ (M = Ni, Co, Fe, Mn, Cr) and of the mixed crystals proved that they crystallize in the same space group. The maximal variations of the edge lengths are 0.7 Å (*a*), 0.2 Å (*b*), and 0.01 Å (*c*), that is, less than 5% of the total value. Therefore, we feel justified to use the interionic distances of $[(C_5Me_5)_2Co]^+$ $[PF_6]^-$ for the evaluation of the intermolecular dipolar signal shifts discussed below. A more detailed description of the structure, which is needed for the calculation of the dipolar NMR signal shifts, is given in the Supporting Information.

Discussion

Spin Distribution in $[(C_5Me_5)_2M]^+$. The experimental NMR signal shifts, δ^{exp}, of paramagnetic molecules are composed of two contributions: the diamagnetic contribution, δ^{dia}, which is due to the shielding by closed-shell electrons, and the paramagnetic contribution, δ^{para}, which is due to the interaction of the nuclear spin with the mean magnetic moment of the electron spin.[17] The paramagnetic signal shifts depend on the absolute temperature, *T*, and are hence usually reported as $\delta^{para}{}_T$. Since the spectra were recorded at slightly different temperatures, mostly a few degrees above room temperature, all data were converted to signal shifts at the standard temperature 298 K by following the relation $\delta^{para} \propto T^{-1}$. The shifts summarized in Table 2 are $\delta^{para}{}_{298}$ values that allow proper comparison.

The paramagnetic signal shift, in turn, is composed of a through-bond contribution, the contact shift, δ^{con}, and a through-space contribution, the dipolar shift, δ^{dip}. Because only δ^{con} is proportional to the spin density, δ^{dip} must be subtracted from δ^{para}. In the Supporting Information, it is shown that δ^{dip} is small in most cases so that the data of Table 2 reflect the spin densities except for cases that are discussed below. In particular, the δ^{para} values of the five-ring carbon atoms correspond to the spin densities in the π orbitals at the ligands. Obviously (Table 2), this spin density is positive for $[(C_5Me_5)_2Ni]^+$ and negative for $[(C_5Me_5)_2Cr]^+$ and $[(C_5Me_5)_2Mn]^+$ in accordance with solution-state data. It has been shown previously that the corresponding signal shifts of ferrocenium ions in solution are contaminated by large positive dipolar shifts (230−320 ppm).[11] When these are removed, the remaining contact shift, and thus the spin density in the ligand π orbitals, is negative. Whether this π spin density is positive or negative depends on the delocalization mechanism:[17c] If the metal d-electron count is $d > 6$, direct metal−ligand spin transfer yields positive spin density because the unpaired electrons are in MOs which have considerable ligand contents (cf. Figure 1a, site **A′**). If the electron count is $d < 6$, the unpaired electrons are in MOs which are essentially metal orbitals, so that polarization of the metal−ligand bonding electrons yields negative spin density (cf. Figure 1c, site **B′**). When the NMR data in Table 2 are compared with the experimental findings[20] and to the theoretical model,[10c,d,g] perfect agreement is found: The spin density in the ligand π orbitals of the cations $[(C_5Me_5)_2M]^+$ is negative for M = Cr, Mn, and Fe, and ferromagnetic interaction is found (cf. Figure 1d) for the $[TCNE]^-$ salts. In contrast, for M = Ni the corresponding spin density is positive, and the interaction with $[TCNE]^-$ is antiferromagnetic (cf. Figure 1b).

Quantitative information on the spin distribution in metallocenium ions is obtained from the spinning sideband patterns associated with the isotropic signals of the five-ring carbon atoms. The total chemical shift tensor of a NMR signal of a paramagnetic compound comprises the diamagnetic shift tensor, the anisotropic hyperfine interaction tensor (due to dipolar interactions with electron spin density in a p, d, and f orbital at the atom under consideration[21]), and the dipolar interactions between the nucleus and the electron spin density located at remote positions.[22] All tensor contributions of the ring carbon signals of the cations $[(C_5Me_5)_2M]^+$ are axially symmetric with

Table 2. Paramagnetic Shifts[a] and Half-Widths[b] of the Isotropic ^1H, ^{13}C, ^{31}P, and ^{19}F MAS NMR Signals of Solid Decamethylmetallocenium $[TCNE]^-$ and $[PF_6]^-$ Salts Compared to the Paramagnetic Signal Shifts of Corresponding $[PF_6]^-$ Salts in Acetone Solution

compound	C_{ring}	CH_3	H	P	F
$[(C_5Me_5)_2Ni]^+$ $[PF_6]^-$	519	−227	98	10.8	10.7
	(0.8)	(0.4)	(0.9)	(0.4)	(0.5)
solution	528	−250	102		
$[(C_5Me_5)_2Co]^+$ $[TCNE]^-$	26.3	18.8	0.7		
	(0.3)	(0.2)	(0.7)		
$[(C_5Me_5)_2Fe]^+$ $[PF_6]^-$	173	−25	−30	−12.5	−13.0
	(2.7)	(2.7)	(10)	(4.8)	(8.0)
solution	165	−29	−39		
$[(C_5Me_5)_2Fe]^+$ $[TCNE]^-$	194	−15	−42		
	(2.1)	(2.0)	(6.7)		
$[(C_5Me_5)_2Mn]^+$ $[PF_6]^-$	−108	572	−57	−13.5	−13.4
	(2.4)	(2.4)	(6.7)	(4.1)	(4.8)
solution	−118	580	−64		
$[(C_5Me_5)_2Mn]^+$ $[TCNE]^-$	−79	602	−60		
	(1.3)	(1.3)	(3.4)		
$[(C_5Me_5)_2Cr]^+$ $[PF_6]^-$	−410	818	12	−0.3	−0.8
	(10.0)	(10.0)	(4.1)	(1.7)	(3.5)
solution	−434	830	4		
$[(C_5Me_5)_2Cr]^+$ $[TCNE]^-$	−392	846	8		
	(0.9)	(0.6)	(1.1)		

[a] In ppm at 298 K relative to the diamagnetic signal shifts of solid $[(C_5Me_5)_2Co]^+$ $[PF_6]^-$. [b] In kHz in parentheses.

(17) (a) *NMR of Paramagnetic Molecules*; LaMar, G. N., Horrocks, W. DeW., Jr., Holm, R. H., Eds.; Academic Press: New York, 1973. (b) Drago, R. S. *Physical Methods for Chemists*; Saunders College Publishing: Ft. Worth, TX, 1992; Chapter 12. (c) Köhler, F. H. in ref 2c, p 379−430.

(18) Wang, X.; Liable-Sands, L. M.; Manson, J. L.; Rheingold, A. L.; Miller, J. S. *J. Chem. Soc., Chem. Commun.* **1996**, 1979−1980.

(19) Darkwa, J.; Richardson, J. F.; Sorensen, T. S. *Acta Crystallogr., Sect. C* **1990**, *46*, 745−747.

(20) Miller, J. S.; Epstein, A. J. *Angew. Chem., Int. Ed. Engl.* **1994**, *33*, 385−415.

(21) Morton, J. R.; Preston, K. F. *J. Magn. Reson.* **1978**, *30*, 577−582.

Table 3. Results of the Herzfeld−Berger Analyses Obtained for the ^{13}C MAS NMR Signals of the Five-Ring Carbon Atoms of Metallocenium Cations

compound	T [K]	ν_{rot} [kHz]	δ^{iso}	$\Delta\delta^{a}$	η^{b}	$\Delta\delta^{parac}$	$\Delta\vartheta^{para}{}_{298}{}^{d}$	$\rho_p{}^{e}$ [%]
$[(C_5Me_5)_2Ni]^+$ $[PF_6]^-$	310.5	14.5	590	1091	0.43	1205	1254	3.6
	304.5	12.0	601	1176	0.36	1290	1318	
	310.5	9.5	609	1175	0.31	1289	1302	
$[(C_5Me_5)_2Fe]^+$ $[PF_6]^-$	298.5	5.0	269	223	0.281	337	338	*f*
$[(C_5Me_5)_2Mn]^+$ $[PF_6]^-$	300	6.0	−14	−237	0.35	−123	−124	−1.3
$[(C_5Me_5)_2Cr]^+$ $[TCNE]^-$	293.6	5.0	−308	−153	0.65	39	38	−1.1

[a] $\Delta\delta = \delta_{zz} - (\delta_{xx} + \delta_{yy})/2$. [b] $\eta = (\delta_{yy} - \delta_{xx})/(\delta_{zz} - \delta_{iso})$ with the tensor main values $|\delta_{zz} - \delta_{iso}| \geq |\delta_{xx} - \delta_{iso}| \geq |\delta_{yy} - \delta_{iso}|$. [c] $\Delta\delta^{para}{}_T = \Delta\delta - \Delta\delta^{dia}$. [d] $\Delta\vartheta^{para}{}_{298} = \Delta\delta^{para}{}_T \cdot T/298$ K. [e] ρ_p is the spin density in one carbon p orbital of the ligand (see eq 2). For the calculation of ρ_p the following geometric parameters were taken: $[(C_5Me_5)_2Ni]^+$:[18] rM = 2.105 Å, r_C = 1.42 Å, β = 35.0°, $[(C_5Me_5)_2Mn]^+$ (crystal structure not available, estimated values): r_M = 2.1 Å, r_C = 1.4 Å, β = 35°, $[Cp^*{}_2Cr]^+$:[19] rM = 2.15 Å, r_C = 1.42 Å, β = 33.3°. [f] Not calculated, see text.

respect to the main molecular axis because the cations are rotating rapidly about their 5-fold symmetry axis. In this case, the total shift tensor is given by the isotropic shift and the total shift anisotropy, $\Delta\delta$ ($\Delta\delta = \delta_{||} - \delta_{\perp}$). The latter has diamagnetic and paramagnetic contributions, $\Delta\delta^{dia}$ and $\Delta\delta^{para}$, respectively, and is given as[5c]

$$\Delta\delta = \Delta\delta^{dia} + \Delta\delta^{para} = \Delta\delta^{dia} + \Delta\delta^{hf} + \Delta\delta_M{}^{dip} + 2\cdot\Delta\delta_C{}^{dip} \quad (1)$$

Here, $\Delta\delta^{hf}$ is the anisotropy of the hyperfine interaction tensor, and $\Delta\delta_M{}^{dip}$ and $\Delta\delta_C{}^{dip}$ are the anisotropies of the dipolar interaction tensors associated with spin density at the metal center and at the two neighboring ring carbon atoms, respectively. If the π spin density of a metallocenium ion is positive, the two leading terms, $\Delta\delta^{hf}$ and $\Delta\delta_M{}^{dip}$, have the same sign, thus giving rise to a large total shift anisotropy. If the π spin density is negative, these terms have opposite signs, and the total shift anisotropy is small. For metallocenium ions with known geometry and small *g*-tensor anisotropy, the spin density, ρ_p, in one p orbital of the pentamethycyclopentadienyl ligand can be calculated:[5c]

$$\rho_p = \left[\frac{\Delta\delta^{para}}{C} - 1.5r_M^{-3}(3\cos^2\beta - 1)\right] \Big/ [1.2\langle r_p^{-3}\rangle - 15r_M^{-3}(3\cos^2\beta - 1) - 3r_C^{-3}] \quad (2)$$

In eq 2, r_M is the distance between a ring carbon atom and the metal, r_C is the distance between two neighboring ring carbon atoms, β is the angle between the vector r_M and the 5-fold axis of the metallocenium ion, and $<r_p^{-3}>$ is the expectation value of r^{-3} of the p orbital (for the carbon atom $<r_p^{-3}>$ is 13.5 Å^{-3} [21]), and the constant C (in ppm·Å^3) is given by

$$C = 10^{36}\cdot\left(\frac{\mu_0}{4\pi}\right)\cdot\frac{\beta_e^2\cdot S(S+1)\cdot g_{av}^2}{3kT} \quad (3)$$

In eq 3, μ_0 is the vacuum permeability, β is the Bohr magneton, S is the electron spin quantum number, g_{av} is the mean g factor, k is the Boltzmann factor, and T is the absolute temperature. A Herzfeld−Berger spinning sideband analysis[13] was carried out for the ring carbon signals of four decamethylmetallocenium ions, among them $[(C_5Me_5)_2Ni]^+$ $[PF_6]^-$ at three different spinning rates, ν_{rot}. As can be seen in Figure 11, the agreement between experimental and fitted spectra is good. From Table 3, it follows that the fitting parameters are quite reliable; for instance, the deviation of the paramagnetic shift anisotropy $\Delta\vartheta^{para}{}_{298} = \Delta\delta^{para}{}_T\cdot T/298$ K obtained from the three spectra of $[(C_5Me_5)_2Ni]^+$ is only 2.9% of the mean value of 1291 ppm. From $\Delta\vartheta^{para}{}_{298}$ and eq 2 the electron spin density in one p orbital of the ring carbon atoms of $[(C_5Me_5)_2Ni]^+$ is calculated to be 3.6% of the unpaired electron. This is in keeping with multiple scattering Xα calculations which gave a value of 4.1% for the parent nickelocenium ion.[23] There is a deviation of the shift tensors from total axial symmetry that can be ascribed to a small *g*-factor anisotropy (neglected in this approach), to dipolar carbon-proton coupling, and to distortions due to susceptibility mismatch.[24]

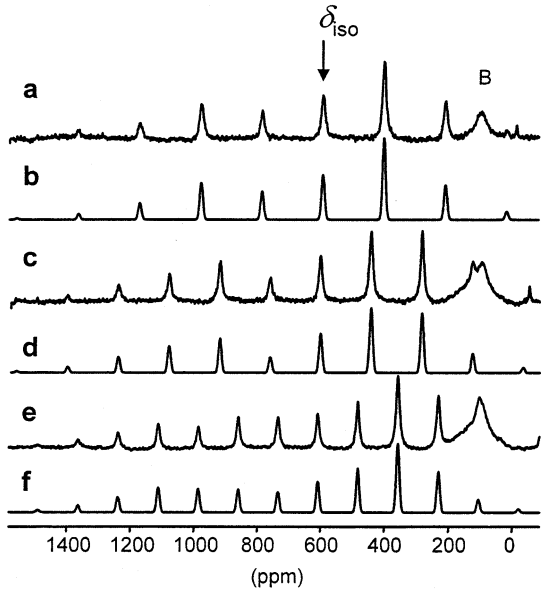

Figure 11. ^{13}C MAS NMR spectra (a, c, e) and simulated spectra (b, d, f) of $[(C_5Me_5)_2Ni]^+$ $[PF_6]^-$ at spinning rates of 14.5 kHz (a and b), 12 kHz (c and d), and 9.5 kHz (e and f). Temperatures: 310 K (a), 305 K (c), and 301 K (e). The isotropic signal (at the center of mass of the anisotropic signal) is marked by an arrow, B is the background signal of the probehead.

For $[(C_5Me_5)_2Fe]^+$, $[(C_5Me_5)_2Mn]^+$, and $[(C_5Me_5)_2Cr]^+$ the total shift anisotropies are significantly smaller than for $[(C_5Me_5)_2Ni]^+$ (Table 3), so that spinning sideband analyses had to be carried out for MAS NMR spectra obtained at low spinning rates. Negative spin densities in the ligand π orbitals were calculated from the shift tensor anisotropies for $[(C_5Me_5)_2Cr]^+$ and $[(C_5Me_5)_2Mn]^+$, as expected for a sandwich compound with less than six d electrons (vide supra). For the cations mentioned

(22) (a) Brough, A. R.; Grey, C. P.; Dobson, C. M. *J. Am. Chem. Soc.* **1993**, *115*, 7318−7327. (b) Nayeem, A.; Yesinowski, J. P. *J. Chem. Phys.* **1988**, *89*, 4600−4608. (c) Kolbert, A. C.; Vesel, R.; De Groot, H.; Almeida, M. *Mol. Phys.* **1997**, *91*, 725−730.

(23) Goursot, A.; Penigault, E.; Weber, J. *New J. Chem.* **1979**, *3*, 675−681.

(24) Grey, C. P.; Dobson, C. M.; Cheetham, A. K. *J. Magn. Reson.* **1992**, *98*, 414−420.

so far, the *g*-factor anisotropy is small[25a,b] so that the analysis is a good approximation.[5c] A different case is the cation $[(C_5Me_5)_2Fe]^+$ where the *g*-factor anisotropy is large and where the quantitative analysis is hampered because additional anisotropic shift contributions come into play. However, the result agrees well with the fact that the paramagnetic shift anisotropy of $[(C_5Me_5)_2Fe]^+$ $[PF_6]^-$ is only about one-fourth of that of $[(C_5Me_5)_2Ni]^+$ $[PF_6]^-$ (while both have $S = 1/2$). This is in line with the fact that negative and positive spin densities on the ligands cause small and large shift anisotropies, respectively. Independently, the analysis may be restricted to the isotropic signal shifts. For the $[PF_6]^-$ salt, a mean dipolar shift of 348 ppm is calculated (eq SI1, Supplementary Information) with $g_{||}^2 - g_\perp^2 = 17.8 - 18.5$[25c] and the distances Fe−C = 2.09 Å and C−C = 1.40 Å.[26] Subtraction from the shift value given in Table 2 yields a contact shift of −175 ppm, which corresponds to the solution-state data[11] and qualitatively shows that the spin in the ligand π orbitals is again negative.

Cation−Cation Interaction in Solid $[(C_5Me_5)_2M]^+$ $[PF_6]^-$. The X-ray powder diffractograms of the mixed crystals $[(C_5Me_5)_2M_xCo_{1-x}]^+$ $[PF_6]^-$ (M = Cr, Ni) showed only one set of reflexes, thus indicating that the different cations are randomly distributed within the crystal lattice and not in separated domains. As can be seen from Figures 4−9 and Tables 1 and 2, the paramagnetic ^{1}H and ^{13}C NMR signal shifts of all $[(C_5Me_5)_2M]^+$ cations are influenced by adjacent cations in the lattice. For $[(C_5Me_5)_2M]^+$ $[PF_6]^-$ in the solid state and in acetone solution the paramagnetic signal shifts differ by amounts of up to 25 ppm, while the deviations of the corresponding diamagnetic signal shifts are below 1 ppm. These differences can have two origins: First, the geometry of the cations in the solid state are likely to differ to some extent from those of dissolved cations, causing a change of the intramolecular spin distribution. A related example is the effect of the host lattice on the spin distribution in cobaltocene which has been disclosed by ENDOR spectroscopy.[27] Second, the influence of adjacent paramagnetic cations in the crystal lattice can contribute to the total NMR signal shifts as well. A selective probe of the latter shift contributions are the MAS NMR signals of the $[(C_5Me_5)_2Co]^+$ cation in the mixed crystals $[(C_5Me_5)_2Ni_xCo_{1-x}]^+$ $[PF_6]^-$ and $[(C_5Me_5)_2Cr_xCo_{1-x}]^+$ $[PF_6]^-$ (Figure 8), where the methyl carbon atoms showed the most pronounced effect. For $[(C_5Me_5)_2Ni_xCo_{1-x}]^+$ $[PF_6]^-$ and $[(C_5Me_5)_2Cr_xCo_{1-x}]^+$ $[PF_6]^-$ the interionic paramagnetic signal shifts caused by each of the two nearest cations were 6.9 ppm and −4.4 ppm, respectively. Origins of the shifts that must be discussed are intermolecular transfer of spin density and dipolar interactions resulting in intermolecular contact shifts and dipolar shifts, respectively.

The intermolecular dipolar shifts are composed of ligand- and metal-centered contributions whose calculation is described in the Supplementary Information. The total dipolar shift amount of the methyl carbon atoms of $[(C_5Me_5)_2Co]^+$ in the mixed crystals of $[(C_5Me_5)_2Ni_xCo_{1-x}]^+$ $[PF_6]^-$ and $[(C_5Me_5)_2Cr_xCo_{1-x}]^+$ $[PF_6]^-$ is less than 0.3 ppm. Therefore, the shifts of 6.9 ppm and −4.3 ppm are intermolecular contact shifts which are ascribed to spin transfer from the $[(C_5Me_5)_2Ni]^+$ and $[(C_5Me_5)_2Cr]^+$ cations, respectively, to $[(C_5Me_5)_2Co]^+$. The solid-state structure (Figure 10) suggests that spin density is transferred from the ligand π orbitals of one metallocenium cation to the methyl groups of the next. Since the spin in the ligand π orbitals of $[(C_5Me_5)_2Ni]^+$ and $[(C_5Me_5)_2Cr]^+$ is positive and negative, respectively (see previous section), both cations must produce intermolecular contact shifts with different signs. This has actually been observed.

So far, the effect on the signal shifts of $[(C_5Me_5)_2Co]^+$ has been discussed. As for $[(C_5Me_5)_2Ni]^+$, dilution by $[(C_5Me_5)_2Co]^+$ results in a low-frequency shift of its methyl carbon signals (Figure SI7). The same was found for pure $[(C_5Me_5)_2Ni]^+$ $[PF_6]^-$ when passing from the solid state to solution (Table 2). Unfortunately, no signal splittings could be observed for other paramagnetic cations because of large signal widths. Nevertheless, it is reasonable to suggest that other signal shift differences for solution and the solid state seen in Table 2 are to a large extent due to intermolecular spin transfer. Intermolecular contact shifts have been observed previously for rare-earth compounds[28] in the solid state and for noncoordinating ion pairs such as $[(nC_4H_9)N]^+_2$ $[MX_4]^{2-}$ in solution and in molten salts.[29]

Cation−Anion Interaction in Solid $[(C_5Me_5)_2M]^+$ $[PF_6]^-$. The ^{19}F and ^{31}P MAS NMR signals of $[(C_5Me_5)_2M]^+$ $[PF_6]^-$ were also shifted when paramagnetic metallocenium cations were present. Studies of the mixed crystals (Figures 9 and SI7) show signal splitting patterns, which are expected when two paramagnetic cations contribute to the signal shifts. The crystal structure (Figure 10) reveals that there are two next-neighbor cations in the *ac* plane of the unit cell.

Calculation of the ligand- and metal-centered intermolecular dipolar shifts including the nearest eight $[(C_5Me_5)_2M]^+$ cations (Supplementary Information) gave 0.4, 5.8, −15.8 ppm, and 0 ppm for M = Cr, Mn, Fe, and Ni, respectively (Table SI3). It is concluded that in the case of nickel the average ^{31}P NMR signal shift of 5.8 ppm (Table 1) per paramagnetic cation in $[(C_5Me_5)_2Ni_xCo_{1-x}]^+$ $[PF_6]^-$ is a contact shift and that this proves spin density transfer from $[(C_5Me_5)_2M]^+$ to $[PF_6]^-$. The signal shift of 10.8 ppm for pure $[(C_5Me_5)_2Ni]^+$ $[PF_6]^-$ (Table 2) is in line with these results. In $[(C_5Me_5)_2Fe]^+$ $[PF_6]^-$ and $[(C_5Me_5)_2Cr]^+$ $[PF_6]^-$ the experimental and dipolar shifts are similar, so that cation−anion spin transfer is less clear. By contrast, in $[(C_5Me_5)_2Mn]^+$ $[PF_6]^-$ subtraction of the dipolar shift from the experimental shift yields a contact shift of −19.3 ppm. Thus, the ^{31}P contact shift is negative when the spin density in the ligand π orbitals is negative and vice versa. This is in keeping with the ^{13}C NMR results and the fact that the ligand π orbitals of the two nearest $[(C_5Me_5)_2M]^+$ cations point toward the $[PF_6]^-$ anion (Figure 10), thereby favoring cation−anion spin transfer.

(25) (a) Nickelocenium and chromocenium ions: Ammeter, J. H. *J. Magn. Reson.* **1978**, *30*, 299−325 and ref 6. (b) Since no data for manganocenium ions are available, the isoelectronic chromocene serves for an estimate: König, E.; Schnakig, R.; Kanellakopulos, B.; Klenze, R. *Chem. Phys. Lett.* **1977**, *50*, 439−441. (c) Duggan, D. M.; Hendrickson, D. N. *Inorg. Chem.* **1975**, *14*, 955−970. (d) Materikova, R. B.; Babin, V. N.; Solodovnikov, S. P.; Lyatifov, A. T.; Petrovsky, P. V.; Fedin, E. I. *Z. Naturforsch., B* **1980**, *35*, 1415−1419.

(26) Reis, A. H., Jr; Preston, D. L.; Williams, J. M.; Peterson, S. W.; Candela, G. A.; Swartzendruber, L. J.; Miller, J. S. *J. Am. Chem. Soc.* **1979**, *101*, 2756−2758.

(27) Rudin, M.; Fauth, J. M.; Schwaiger A.; Ernst, R. R.; Zoller, L.; Ammeter, J. H. *Mol. Phys.* **1983**, *49*, 1257−1275.

(28) (a) Grey, C. P.; Dobson, C. M.; Cheetham, A. K.; Jakeman, R. J. B *J. Am. Chem. Soc.* **1989**, *111*, 505−511. (b) Brough, A. R.; Grey, C. P.; Dobson *J. Am. Chem. Soc.* **1993**, *115*, 7318−7327.

(29) (a) Fritz, H. P.; Gretner, W.; Keller, H. J.; Schwarzhans, K. E. *Z. Naturforsch., B* **1970**, *25*, 174−176. (b) Brown, D. G.; Drago, R. S. *J. Am. Chem. Soc.* **1970**, *92*, 1871−1875. (c) Lim, Y.-Y.; Drago, R. S. *J. Am. Chem. Soc.* **1972**, *94*, 84−90. (d) Bertini, I.; Luchinat, C.; Borghi, E. *Inorg. Chem.* **1981**, *20*, 306−308.

The ^{19}F MAS NMR spectra of the $[(C_5Me_5)_2M]^+$ $[PF_6]^-$ salts showed equivalent fluorine atoms, which means that the $[PF_6]^-$ anions are rotating fast on the NMR time scale. We have not calculated motionally averaged intermolecular dipolar ^{19}F NMR shifts, but it can be assumed that they are similar to the dipolar ^{31}P NMR shifts. Then the signs and the magnitudes of the ^{19}F NMR data in Table 2 confirm that the $[PF_6]^-$ anions receive spin density from paramagnetic $[(C_5Me_5)_2M]^+$ cations at least for M = Cr and Ni.

The transferred spin density of a given nucleus N, $\rho(N)$, can be calculated from the contact shifts, δ^{con}, by[17c]

$$\rho(N) = 9kT\delta^{con}/[\mu_0 g_{av}^2 \beta_e^2 a_0^3 (S+1)] \quad (4)$$

All symbols have been mentioned above except for a_0, which is the Bohr radius. For an estimate, it is assumed that the signal shifts are pure contact shifts and that g_{av} is 2. In $[(C_5Me_5)_2Ni]^+$ $[PF_6]^-$, ^{19}F and ^{31}P NMR signal shifts of about 10 ppm (Table 2) and $S = 1/2$ yield $\rho(^{19}F) \sim \rho(^{31}P) \sim 8\cdot10^{-5}$ atomic units.

Anion−Cation Interaction in $[(C_5Me_5)_2M]^+$ $[TCNE]^-$. A good indication of the interaction between the ions of $[(C_5Me_5)_2M]^+$ $[TCNE]^-$ is the nuclear relaxation. As can be seen in Figure 5, the radical anion $[TCNE]^-$ broadens the ^{13}C MAS NMR signals of the diamagnetic cation $[(C_5Me_5)_2Co]^+$. More strikingly, when the cation $[(C_5Me_5)_2M]^+$ is also paramagnetic, the nuclear relaxation is slowed by electron spin exchange,[30] and the signals become much narrower (Figure 4 and Table 2). This has been observed previously for metallocenes after linking them by covalent bonds,[31] whereas in the present cases interionic interaction is responsible.

All attempts to detect the ^{13}C NMR signals of $[TCNE]^-$ were unsuccessful even for $[(C_5Me_5)_2Cr]^+$ $[TCNE]^-$ whose nuclear relaxation is most favorable. From the spin density distribution in $[TCNE]^-$,[12b] it can be estimated that the signal shift and its anisotropy (see eq 2) would prohibit detection of the sp^2 but not the sp carbon atom.[32] However, even for the latter carbon atoms nuclear relaxation is still too fast. So, there is no direct proof for the delocalization of spin density from a paramagnetic cation to $[TCNE]^-$. Yet, the delocalization should exist by analogy to $[(C_5Me_5)_2M]^+$ $[PF_6]^-$.

Clear evidence for the transfer of spin density from $[TCNE]^-$ to the counterion was found for $[(C_5Me_5)_2Co]^+$ $[TCNE]^-$. The two ^{13}C NMR signals of the cation (Figure 5) were shifted by 26.3 and 18.8 ppm, and these shifts were temperature-dependent (Figure SI6). As expected from positive spin in the antibonding π orbital of $[TCNE]^-$, the sign of these shifts is positive. Unlike in the preceding two sections, intermolecular dipolar shifts can be neglected here, because the *g*-factor anisotropy (cf. eq SI1, Supplementary Information) is generally very small for organic radicals. Thus, spin density of up to $2\cdot10^{-4}$ au per carbon atom is delocalized to $[(C_5Me_5)_2Co]^+$. About the same transfer of positive spin density from $[TCNE]^-$ to the cations $[(C_5Me_5)_2M]^+$ occurs when they are paramagnetic (M = Cr, Mn, and Fe). This was calculated from the shift differences of 10−30 ppm between the ^{13}C NMR signals of the $[TCNE]^-$ and $[PF_6]^-$ salts by using eq 4.

Conclusions

It has been shown that solid-state NMR spectroscopy is the method of choice for studying the mechanism that mediates magnetic interaction in molecule-based magnetic materials of the type metallocenium tetracyanoethenide. It provides information on the spin distribution, which cannot be obtained from solution NMR spectra.

The analysis of not only the sign but also the anisotropy of the NMR signal shifts of the salts $[(C_5Me_5)_2M]^+$ $[PF_6]^-$ reveals that the spin density in the π orbitals of the (C_5Me_5) ligands is positive when M is Ni and negative when M is Cr, Mn, and Fe. The ions interact with each other as indicated by drastic changes of the relaxation time of the nuclei of both cations and anions. More importantly, the interactions cause changes of the ^1H, ^{13}C, ^{19}F, and ^{31}P MAS NMR signal shifts, most of which establish that the spin density is not restricted to a given ion but transferred in part to neighboring ions. Spin delocalization has been shown to proceed from cation to cation and from cation to anion in $[(C_5Me_5)_2M]^+$ $[PF_6]^-$ and from anion to cation in $[(C_5Me_5)_2M]^+$ $[TCNE]^-$. The results obtained for $[(C_5Me_5)_2M]^+$ $[PF_6]^-$ suggest that reverse spin density transfer also occurs from $[(C_5Me_5)_2M]^+$ to $[TCNE]^-$, although slow electron spin relaxation did not allow detection of NMR signals of $[TCNE]^-$. The transferred spin density is about 10^{-4} au, which would be hard to measure by using polarized neutron diffraction. The sign of the spin density does not change on the delocalization path.

The scenario that emerges from these results matches both requirements of the McConnell-I mechanism: First, the sign of the spin density at the periphery of the cations $[(C_5Me_5)_2M]^+$ in metallocenium salts is in keeping with what was derived with Figures 1 and 2. It is negative when the magnetic interaction in $[(C_5Me_5)_2M]^+$ $[TCNE]^-$ is ferromagnetic and positive when it is antiferromagnetic. Second, in the solid state the ions do interact. All paramagnetic ions experience changes of their spin density through spin transfer from neighboring paramagnetic ions, which points to orbital overlap.

Molecule-based magnetic materials other than the metallocenium derivatives may be studied by solid-state NMR spectroscopy as well if the relaxation time can be adjusted properly. It is expected that tuning of intermolecular spin transfer can be monitored in this way.

Experimental Section

All compounds were prepared by literature methods.[6,7,14,33] Except for pure $[(C_5Me_5)_2Co]^+$ $[PF_6]^-$, they were handled under dry and oxygen-free nitrogen by using Schlenck techniques and solvents that were dried by standard methods and saturated with inert gas. Single crystals of $[(C_5Me_5)_2Co]^+$ $[PF_6]^-$ were grown by slow evaporation from a saturated acetone solution. The mixed crystals $[(C_5Me_5)_2Ni_xCo_{1-x}]^+$ $[PF_6]^-$ with $x = 0.6$ and 0.9 and $[(C_5Me_5)_2Cr_xCo_{1-x}]^+$ $[PF_6]^-$ with $x = 0.3$ and 0.8 were obtained by crystallization from corresponding mixtures of $[(C_5Me_5)_2Ni]^+$ $[PF_6]^-$ and $[(C_5Me_5)_2Co]^+$ $[PF_6]^-$ or $[(C_5Me_5)_2Cr]^+$ $[PF_6]^-$ and $[(C_5Me_5)_2Co]^+$ $[PF_6]^-$ in acetone/hexane solution. The ratios of the metals in the mixed crystals were determined by elemental analyses.

NMR Measurements and Simulations. All NMR spectra were recorded by using a Bruker MSL 300 spectrometer with a 4-mm standard Bruker MAS probehead. ZrO_2 and Si_3N_4 rotors with a diameter

(30) Molin, Yu. N.; Salikhov, K. M.; Zamaraev, K. I. *Spin Exchange*; Oxford University Press: New York, 1980.
(31) Atzkern, H.; Bergerat, P.; Beruda, H.; Fritz, M.; Hiermeier, J.; Hudeczek, P.; Kahn, O.; Köhler, F. H.; Paul, M.; Weber, B. *J. Am. Chem. Soc.* **1995**, *117*, 997−1011.
(32) Heise, H., Ph.D. Thesis, TU München, 1999.
(33) (a) Eichhorn, D. M.; Skee, D. C. Broderick, W. E. Hoffman,B. M. *Inorg. Chem.* **1993**, *32*, 491−492. (b) Duggan, D. E.; Hendrickson, D. N. *Inorg. Chem.* **1975**, *14*, 955−970. (c) Robbins, J. L.; Edelstein, N. M.; Smart, J. C.; Cooper, S. R. *J. Am. Chem. Soc.* **1979**, *101*, 8353−8357.

of 4 mm were packed under inert gas with about 50 mg of the sample and about 10 mg of nickelocene as an internal temperature standard and then were sealed with Kel-F caps. The FIDs were sampled after applying single pulses (duration 4 μs). Delays of 8−10 μs were applied for detector recovery, and repetition times were 200−400 ms for NMR spectra of paramagnetic compounds and 2−4 s for diamagnetic compounds. For the ^{13}C CP MAS NMR spectra of $[(C_5Me_5)_2Co]^+$ $[PF_6]^-$ the contact pulse length was 5 ms. The spectra were improved by line broadening up to the matched filter and by baseline correction. Signal shifts were measured relative to the external secondary standards adamantane (δ (^{1}H) = 2.0 ppm, δ ($^{13}CH_2$) = 29.5 ppm), $(NH_4)H_2PO_4$ (δ (^{31}P) = 1.1 ppm), and NaF (δ (^{19}F) = −224.4 ppm), respectively. The paramagnetic signal shifts of the solids were calculated relative to those of the diamagnetic analogue $[(C_5Me_5)_2Co]^+$ $[PF_6]^-$ ($\delta^{dia}(^{13}C_{ring})$ = 95.3, $\delta^{dia}(^{13}CH_3)$ = 8.1, $\delta^{dia}(^1H)$ = 2.1, $\delta^{dia}(^{31}P)$ = −144.1, $\delta^{dia}(^{19}F)$ = −68.6). The temperature was measured internally for each sample at each spinning rate by observing the calibrated temperature-dependent proton signal shift of nickelocene.[5c] Sideband analyses according to Herzfeld and Berger[13] were carried out with the program Wsolids, HBA 1.2.[34a] MAS NMR spectra with the tensor values obtained by these sideband analyses were simulated with the program Wsolids 1.[34b]

Crystal Structure. A single crystal of $[(C_5Me_5)_2Co]^+$ $[PF_6]^-$ was mounted on a thin glass fiber with viscous oil and then cooled to −74 °C. Crystal data and details of the measurements are summarized in Table 4 (see also Supporting Information). Data were collected on a NONIUS CAD 4 diffractometer using ω-scans. Unit-cell parameters were determined from 100 data frames collected at different sections of the Ewald sphere. Semiempirical absorption corrections based on equivalent reflections were applied. The structure was solved by Patterson methods, completed with difference Fourier syntheses, and refined with full-matrix least-squares procedures based on F^2. All non-hydrogen atoms were treated as idealized contributions. All scattering factors and anomalous dispersion factors are contained in the SHELXTL 5.1 program library.[35]

(34) (a) Eichele, K.; Wasylishen, R. E. *HBA 1.2*; Dalhousie University: Halifax, Canada. (b) Eichele, K.; Wasylishen, R. E. *Wsolids1*; Dalhousie University: Halifax, Canada.
(35) Sheldrick, G. M. Program Package SHELXTL, Version 5.1; Universität Göttingen.

Table 4. Crystal Data and Structure Refinement for $[(C_5Me_5)_2Co]^+$ $[PF_6]^-$

empirical formula	$[CoC_{20}H_{30}]^+$ $[PF_6]^-$
formula weight	474.36
crystal system	monoclinic
space group	*C*2/*m*
color of crystal	yellow
unit cell parameters	
a (Å)	14.0459(9)
b (Å)	8.9028(4)
c (Å)	9.1186(5)
β (deg)	112.724(2)
volume (Å^3)	1051.8(1)
temperature (K)	199(2)
Z	2
R1[a]	0.0332
wR2[b]	0.0905
goodness of fit	1.146

[a] $R1 = \Sigma||F_o| - |F_c||/\Sigma|F_o|$. [b] $wR2 = (\Sigma w(|F_o| - |F_c|)^2/\Sigma w|F_o|^2)^{1/2}$.

Acknowledgment. This work has been supported by the European Union (HCM network "Magnetic Molecular Materials") and by the Fonds der Chemischen Industrie. We thank Dr. E. Herdtweck and L. Jakobsmeier for assistance with the X-ray powder studies.

Supporting Information Available: Variable-temperature ^{13}C MAS NMR spectra of $[(C_5Me_5)_2Ni]^+$ $[PF_6]^-$, ^{1}H and ^{13}C MAS NMR spectra of $[(C_5Me_5)_2Mn]^+$ $[PF_6]^-$ and $[(C_5Me_5)_2Fe]^+$ $[PF_6]^-$, variable-temperature ^{13}C MAS NMR spectra of $[(C_5Me_5)_2Co]^+$ $[PF_6]^-$, ^{13}C, ^{1}H, and ^{31}P MAS NMR spectra of $[(C_5Me_5)_2Ni_xCo_{1-x}]^+$ $[PF_6]^-$, crystal data and structure refinement of $[(C_5Me_5)_2Co]^+$ $[PF_6]^-$ (extended version), positional and thermal atom parameters of $[(C_5Me_5)_2Co]^+$ $[PF_6]^-$, interionic distances of $[(C_5Me_5)_2Co]^+$ $[PF_6]^-$, calculation of interionic dipolar shifts, and X-ray powder data. This material is available free of charge via the Internet at http://pubs.acs.org.

JA020026L